

2012

# Impact of Farm Equipment Loading on Rigid Pavement Performance Using Finite Element Analysis

Shiyun Wang

Iowa State University, [wsy@iastate.edu](mailto:wsy@iastate.edu)

Halil Ceylan

Iowa State University, [hceylan@iastate.edu](mailto:hceylan@iastate.edu)

Sunghwan Kim

Iowa State University, [sunghwan@iastate.edu](mailto:sunghwan@iastate.edu)

Kasthurirangan Gopalakrishnan

Iowa State University, [rangan@iastate.edu](mailto:rangan@iastate.edu)

Lev Khazanovich

University of Minnesota - Twin Cities

*See next page for additional authors*

Follow this and additional works at: [http://lib.dr.iastate.edu/ccee\\_conf](http://lib.dr.iastate.edu/ccee_conf)

 Part of the [Bioresource and Agricultural Engineering Commons](#), and the [Construction Engineering and Management Commons](#)

---

## Recommended Citation

Wang, Shiyun; Ceylan, Halil; Kim, Sunghwan; Gopalakrishnan, Kasthurirangan; Khazanovich, Lev; and Dai, Shongtao, "Impact of Farm Equipment Loading on Rigid Pavement Performance Using Finite Element Analysis" (2012). *Civil, Construction and Environmental Engineering Conference Presentations and Proceedings*. 4.

[http://lib.dr.iastate.edu/ccee\\_conf/4](http://lib.dr.iastate.edu/ccee_conf/4)

This Conference Proceeding is brought to you for free and open access by the Civil, Construction and Environmental Engineering at Iowa State University Digital Repository. It has been accepted for inclusion in Civil, Construction and Environmental Engineering Conference Presentations and Proceedings by an authorized administrator of Iowa State University Digital Repository. For more information, please contact [digirep@iastate.edu](mailto:digirep@iastate.edu).

---

# Impact of Farm Equipment Loading on Rigid Pavement Performance Using Finite Element Analysis

## **Abstract**

The increase in agricultural product sales in recent years has led to the use of larger hauling and application equipment to transfer farm productions. This rapid shift in equipment size has raised a concern about their potential to cause significant damage in pavements and bridges. The study reported in this paper (part of a larger pooled fund study initiated in 2007) discusses the impact of farm equipment loading on rigid pavement performance based on Finite Element (FE) analysis. The study considered various types of farm equipment to determine the pavement responses and to quantify their damage on rigid pavement systems. The ISLAB2005 FE pavement response model was employed for numerical modeling and analysis of the test sections subjected to farm equipment loading. The results of FE analysis demonstrated that the rigid pavement damage caused by farm vehicles is governed by their axle weight rather than the gross vehicle weight. The FE analysis also showed that the damage resulting from farm equipment loading coupled with PCC slab curling could have a devastating effect on concrete pavement performance.

## **Keywords**

farm vehicles, finite element method, load factor, pavement distress, pavement performance, rigid pavements

## **Disciplines**

Bioresource and Agricultural Engineering | Civil and Environmental Engineering | Construction Engineering and Management

## **Comments**

This paper is from *10th International Conference on Concrete Pavements*, Quebec City, Quebec, Canada, July 8-12. p.546-560. Posted with permission.

## **Authors**

Shiyun Wang, Halil Ceylan, Sunghwan Kim, Kasthurirangan Gopalakrishnan, Lev Khazanovich, and Shongtao Dai

## **Impact of Farm Equipment Loading on Rigid Pavement Performance Using Finite Element Analysis**

Shiyun Wang<sup>1</sup>, Halil Ceylan<sup>2</sup>, Sunghwan Kim<sup>3</sup>, Kasthurirangan Gopalakrishnan<sup>4</sup>, Lev Khazanovich<sup>5</sup> and Shongtao Dai<sup>6</sup>

### **Abstract**

The increase in agricultural product sales in recent years has led to the use of larger hauling and application equipment to transfer farm productions. This rapid shift in equipment size has raised a concern about their potential to cause significant damage in pavements and bridges. The study reported in this paper (part of a larger pooled fund study initiated in 2007) discusses the impact of farm equipment loading on rigid pavement performance based on Finite Element (FE) analysis. The study considered various types of farm equipment to determine the pavement responses and to quantify their damage on rigid pavement systems. The ISLAB2005 FE pavement response model was employed for numerical modeling and analysis of the test sections subjected to farm equipment loading. The results of FE analysis demonstrated that the rigid pavement damage caused by farm vehicles is governed by their axle weight rather than the gross vehicle weight. The FE analysis also showed that the damage resulting from farm equipment loading coupled with PCC slab curling could have a devastating effect on concrete pavement performance.

### **Introduction**

Current trend shows that farms are getting fewer, but farm size is becoming larger and larger. As a result, the farm equipment is simultaneously becoming larger to adapt to the new state and federal regulations which encourage farmers to store manure as a liquid and apply it in a short time period. The effect of such an increase on pavements would be an accelerated rate of pavement deterioration. There is a concern that they can do significant damage to pavements and bridges.

A limited number of studies (Fanous et al. 1999, Oman et al. 2001, Sebaaly et al. 2002) appear in the literature addressing the pavement damage issue caused by heavy farm equipment. However, the results of these previous studies were inconclusive in drawing correspondence between farm equipment type and loading to specific pavement distresses. Additionally, there was not enough information available to quantitatively estimate the pavement damage caused by heavy farm equipment.

A pooled fund study was initiated in early 2007 to gain a better understanding of the interaction of farm equipment with the pavement structures in the United States especially in the mid-west region including Minnesota, Iowa, Illinois, and Wisconsin.

<sup>1</sup> Geotechnical Engineer (Former Graduate Student in Iowa State University), Kleinfelder, Tulsa, OK 74116, USA, Email: [SWang@kleinfelder.com](mailto:SWang@kleinfelder.com)

<sup>2</sup> Ph.D., Associate Professor, Iowa State University, Ames, IA 50011, USA, E-mail: [hceylan@iastate.edu](mailto:hceylan@iastate.edu)

<sup>3</sup> Ph.D., Postdoctoral Research Associate, Iowa State University, Ames, IA 50011, USA, Email: [sunghwan@iastate.edu](mailto:sunghwan@iastate.edu)

<sup>4</sup> Ph.D., Research Assistant Professor, Iowa State University, Ames, IA 50011, USA, E-mail: [rangan@iastate.edu](mailto:rangan@iastate.edu)

<sup>5</sup> Ph.D., Associate Professor, University of Minnesota, Minneapolis, MN 55455, USA, E-mail: [khaza001@tc.umn.edu](mailto:khaza001@tc.umn.edu)

<sup>6</sup> Ph.D., Research Operations Engineer, Minnesota Department of Transportation, Maplewood, MN 55109, USA, E-mail: [Shongtao.Dai@dot.state.mn.us](mailto:Shongtao.Dai@dot.state.mn.us)

The overall objectives of this pooled fund study were to determine the pavement responses under various types of agricultural equipment and to compare these responses with a typical 5-axle semi tractor-trailer. A wide combination of vehicle types, axle load magnitudes, speed levels and rear wheel-to-center wander magnitudes was used to determine the effect of farm equipment loading on asphalt and concrete pavements. The instrumented test sections in MnROAD low volume road loop were utilized in the pooled fund study. The detailed discussions regarding field test procedures and findings for this pooled fund study are found elsewhere (Lim et al. 2011). As a further discussion on the impact of farm equipment under different concrete pavement design features and site conditions, this paper employed ISLAB2005 Finite Element (FE) pavement response model to determine the pavement responses and damages on rigid pavement systems resulting from farm equipment loading. The findings from this study are expected to provide highway engineers an improved understanding of pavement design aspects in resisting damage resulting from heavy agricultural vehicle loading, as well as to guide the regulation of farm equipment more rationally.

### Brief Descriptions of PCC Test Sections

The Portland Cement Concrete (PCC) test sections utilized in this study were cells of 32 and 54 in MnROAD low volume road loop. MnROAD is located along Interstate 94, forty miles northwest of Minneapolis/St. Paul, and contains more than 50 test cells on three different segments, including interstate, low volume road, and farm loop. The low volume road is a two-lane, 2.5-mile closed loop. Cells 32 and 54 (highlighted in Figure 1) constructed in 2000 and 2004 were utilized for this study after retrofitting the instrumentation.

Cell 32 representing thin PCC pavements consists of five inch thick concrete slab over a seven inch thick gravel base while cell 54 representing thick PCC pavements consists of 7.5-inch thick concrete slab over a 12-inch thick gravel base. The PCC slab panel lengths are 10 ft. for cell 32 and 15 ft. for cell 54. The PCC slab panel width of both cells is 12 ft. Cell 32 does not have dowel bar but Cell 54 has one-inch dowel in the transverse joints. Granular shoulders were adjacent to both lanes of cell 32 and cell 54. Installed sensors in both cells include strain, pressure and linear variable differential transformers (LVDTs) to measure pavement response under loads. The detailed descriptions of instrumentation in both cells are provided in Lim et al. (2011) and Wang (2011).

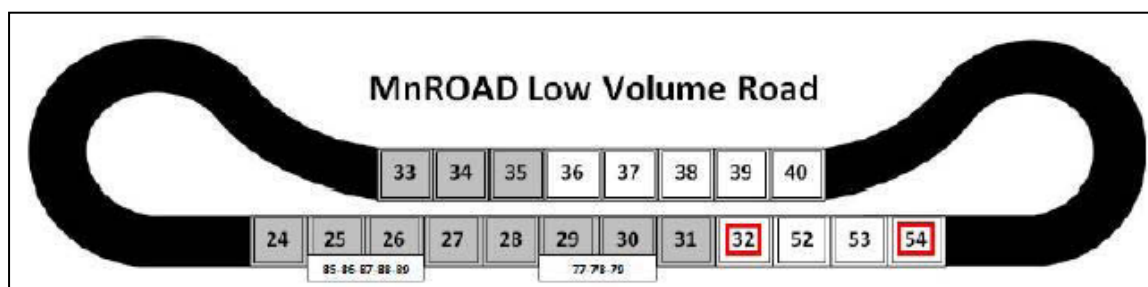


**Figure 1. Cell 32 and cell 54 at MnROAD low volume road (adapted from Snyder 2008)**

### Test Vehicles and Loading conditions

The PCC pavement cells were tested under various types of farm equipment. The trafficking program consisted of subjecting the PCC test cells to several passes of farm vehicles identified for the study as well as a standard five-axle tractor-trailer truck with 80,000-lbs of loading (Mn80). The farm vehicles tested employed two loading conditions: half-loaded (50%) and fully loaded (100%, all water tanks full). The control vehicle, Mn80, was kept at constant weight of 80 kip throughout each testing cycle. All of vehicles run at about 20 mph speed. Table 1 lists the total vehicle weights along with axle loads for five representative vehicles that were tested and analyzed in this paper. These vehicles are grain-cart (G1), terra-gator (R6), straight truck (S5), tanker (T6) and Mn80 (control vehicle). The dimensions of these vehicles are presented in Figure 2. The detailed descriptions of each vehicle are provided in Lim et al. (2011) and Wang (2011)

**Table 1. Total vehicle weights along with axle loads of vehicles tested and analyzed**

Vehicle ID	G1		R6		S5		T6		Mn80
Type / Volume	Grain Cart /1,000 bushels		Terragator /4,200 gal		Straight Truck/4,400 gal		Tanker /6,000 gal		Standar d Semi
Number of Total Axles/Rear Axles	3/1		2/1		3/2		4/2		5/2
Load Level	0%	100%	50%	100%	50%	80%	50%	100%	80-kip
Axle 1 Weight, lbs	12,050	11,500	28,300	32,800	13,280	16,914	8,900	8,100	12,000
Axle 2 Weight, lbs	16,750	18,700	28,700	41,900	14,320	23,337	18,600	21,400	17,000
Axle 3 Weight, lbs	33,850	57,200			15,340	24,339	16,600	26,500	17,000
Axle 4 Weight, lbs							20,300	33,500	16,000
Axle 5 Weight, lbs									18,000
Total Weight, lbs	62,650	87,400	57,000	74,700	42,940	64,590	64,400	89,500	80,000

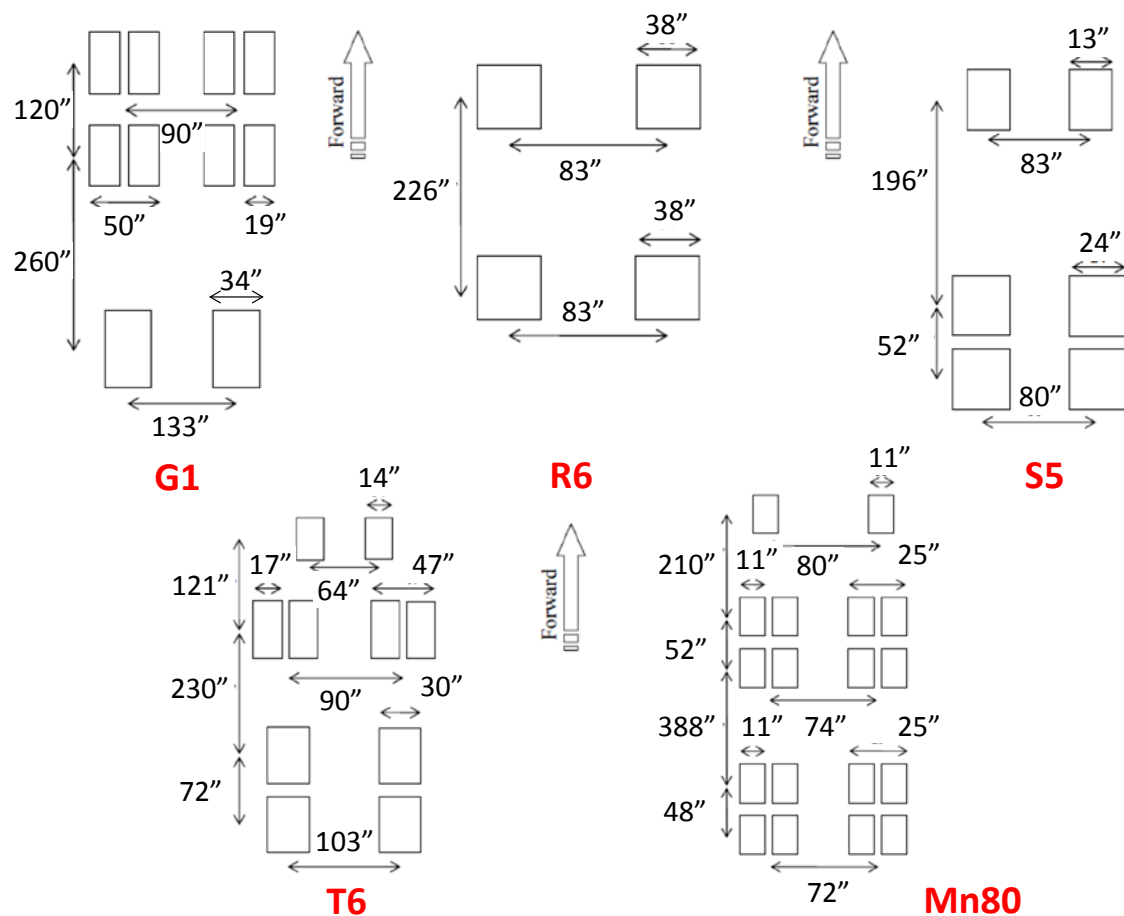


**Figure 2. Dimensions for test vehicles (note: dimension unit - inch; not to scale)**

### Finite Element Modeling

The ISLAB2005 FE rigid pavement analysis model was employed to estimate the pavement responses. The goal was to examine the relative pavement damage potential from various types of farm equipment compared to a standard semi-truck (Mn80). To achieve this objective, the field-measured and FE predicted pavement responses were compared. ISLAB2005 is a FE modeling program developed for predicting rigid pavement responses under traffic and temperature loading (Khazanovich et al. 2005). ISLAB2005 allows the user to manually define the number of the nodes, pavement layers, and complicated wheel configurations and loadings. In the analysis of FE solutions, it the bottom of the slab near mid-slab edge was considered to have critical pavement responses when the heaviest axle loads are near mid-slab edge.

**Comparison of ISLAB2005 Predictions and Field Measurements.** A parametric study was performed by varying the modulus of subgrade support and slab temperature differential to identify proper ISLAB2005 inputs to closely match predicted and measured responses. Farm vehicles, R6, T6 and G1, were selected to examine the accuracy of the ISLAB2005 predictions because these vehicles were identified as having a relatively high risk of damage potential based on field measurement results. The standard MnROAD truck, Mn80, was also included as a control vehicle.

In the FE modeling, the slab width was set to 12 ft. and the slab length was set to 15 ft. for all the simulations to represent cell 54. A mesh size of 6-inch by 6-inch was chosen. The concrete elastic modulus was set at  $4.5 \times 10^6$  psi and the PCC Coefficient of Thermal Expansion (CTE) was set at  $5.5 \times 10^{-6}$  /°F for all the simulation runs. The Load Transfer Efficiency (LTE) for the x-direction (perpendicular to traffic direction) was set at 40% while it was set at 50% for the y-direction (traffic direction).

The modulus of subgrade reaction (k) and slab temperature differences ( $\Delta T$ ) were varied as follows:

- Modulus of subgrade reaction (psi/in.): 50, 100, 200, 300
- Slab Temperature Differences (°F): 40, 30, 20, 10, 0, -10, -20, -30, -40

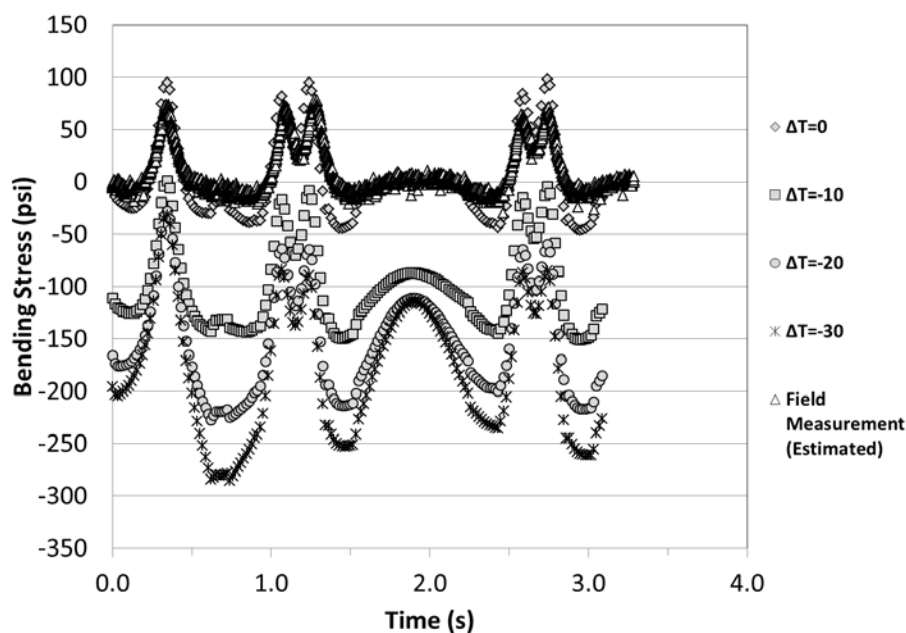


**Figure 3. Comparison of ISLAB2005 and field measured bending stresses at the bottom of the PCC slab near mid-slab edge (Mn80 truck, k = 200 psi/in)**

To simulate the dynamic loading effect on critical pavement stress responses at the mid-slab bottom edge, the loading position of the each vehicle began as the first axle of the vehicle touches the beginning of the slab and then was moved along the traffic direction every 5 inches until the last axle of the vehicle leaves the slab. Figure 3 compares the bending stress at the bottom of the PCC slab near mid-slab edge obtained from FE solutions and field measurements for Mn80 truck loading. Note that the bending stress responses of field measurements in Figure 3 were estimated from an assumed relationship between elastic modulus and strain measurements which were obtained from the strain sensor installed near mid-slab bottom edge in cell 54.

For these comparisons, the k-value is set at 200 psi/in. It is seen that the closest match between FE predictions and field measurements is observed under no temperature difference condition. This result agrees with the previous findings derived from the parametric study for other vehicles. Some magnitude differences in

peak bending stress comparisons were observed. These differences may be due to a number of reasons. The bending stress of field measurements were estimated under assumptions based on strain reversals and no residual thermal strain prior to load. Those assumptions do not properly account for actual curling strain and stress measurements. The assumptions used in FE model for simplifying actual field condition could be one of the reasons.

***Effect of Joint Spacing on Bending Stresses.*** Slab length is one of the most significant factors affecting pavement service life and construction cost. Although longer slab with fewer saw cuts could reduce the construction cost, there is a general increasing probability of developing a transverse crack sooner for increasing slab length. It has been recognized that shorter slab length would increase the effectiveness of aggregate interlock and thus provide a longer service life (De Young 1966).

Three different slab lengths, 10, 15, and 20 ft., were used to estimate the maximum bending stress induced by various farm equipment. The slab thickness, modulus of subgrade reaction, elastic modulus of the concrete pavement, and Poisson's ratio were set as 7 in., 200 psi/in,  $4.5 \times 10^6$  psi, and 0.15, respectively. Figure 4 presents the maximum bending stress predictions at the bottom of the PCC slab near mid-slab edge produced by the five representative test vehicles under various slab length conditions.

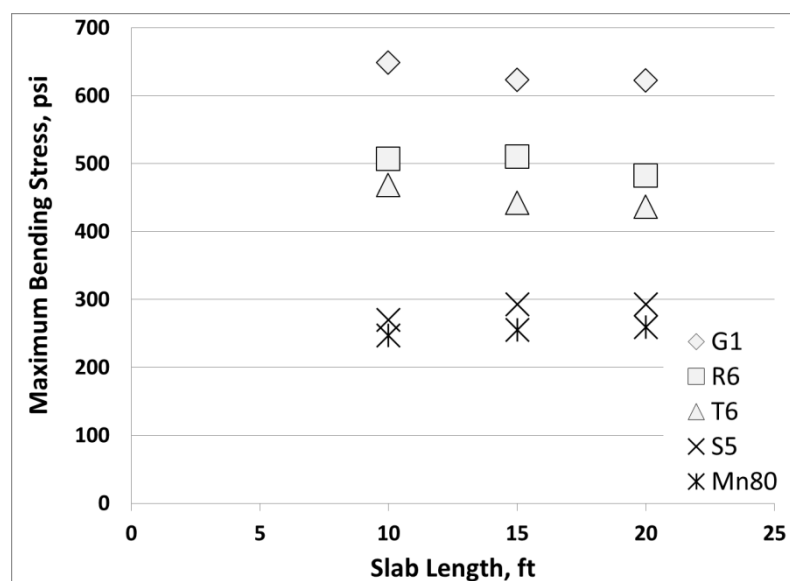


**Figure 4. Effect of slab length on maximum bending stress at the bottom of the PCC slab near mid-slab edge**

All four farm vehicles evaluated in this study produced higher bending stress than the standard semi-truck, Mn80. Among the four farm vehicles, G1 produced the highest bending stress while S5 produced slightly higher bending stress than Mn80. The correlation between slab length and maximum bending stress appeared to vary by vehicle's configuration. Maximum bending stress decreased as slab length increased for G1, R6 and T6. However, this observation was not true for S5 and Mn80.

***Effect of Modulus of Subgrade Reaction on Bending Stresses.*** The modulus of subgrade reaction (k-value) is a key factor in rigid pavement design. In this study, the

k-values investigated ranged from 50 to 300 psi/in. for the tested vehicles. Figure 5 displays the maximum bending stress at the bottom of the PCC slab near mid-slab edge produced by test vehicles under various subgrade strength conditions.

As seen in Figure 5, the k-value has a significant effect on the maximum bending stress experienced by the PCC slab. The maximum bending stress of the rigid pavement could be reduced as much as 36% for G1 when the k-value is increased from 50 to 300 psi/in. The effect of higher k-value on pavement bending stress is minimal for T6 while the straight truck and standard semi-truck (Mn80) rank somewhere in the middle.

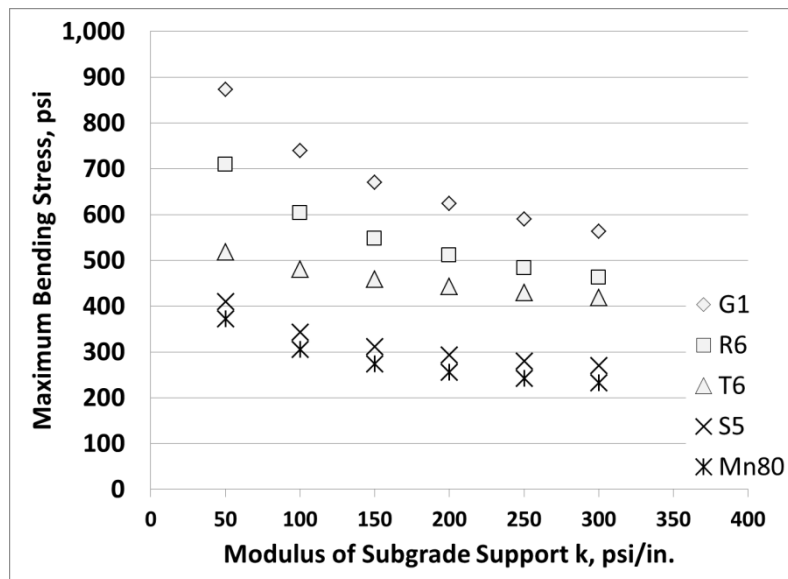


**Figure 5. Effect of modulus of subgrade reaction on maximum bending stress at the bottom of the PCC slab near mid-slab edge**

**Effect of Axle Weight on PCC Slab Stress Ratio.** Although the gross vehicle weight of some farm vehicles are significantly greater than others, their maximum axle weights are not necessarily higher because the heavier loading is distributed into larger tire contact area by having more axles (Wang 2011). The effect of the axle weight on pavement stress ratio for tested vehicles was also investigated. The stress ratio, defined as the ratio of maximum stress ( $\sigma_{max}$ ) at mid-slab edge bottom to the modulus of rupture (MOR) of the concrete, was selected as an evaluation index in this investigation. Fatigue damage is expected to occur to the PCC slab under the number of load repetitions if the stress ratio is over 0.5 (Huang 1993).

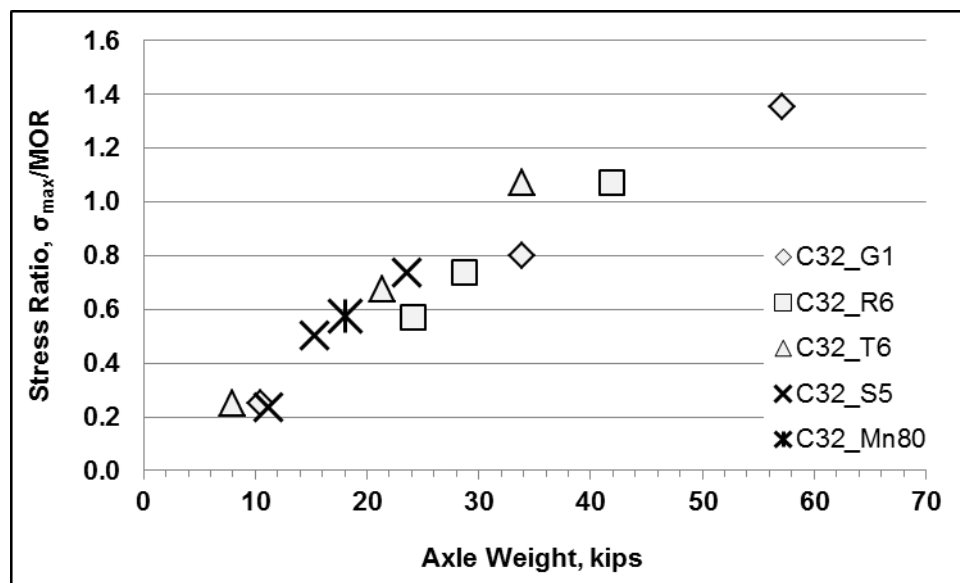


**Figure 6. Effect of vehicle axle weight on PCC slab stress ratio**

Figure 6 shows the correlation between the pavement stress ratio and axle weight for the five test vehicles in cell 32. As seen in Figure 6, there is a linear relationship between the PCC slab stress ratio and the axle weight regardless of vehicle type. A farm vehicle axle weight limit of 18 kips could be recommended if a stress ratio of 0.5 is used as the critical threshold (above which the pavement is likely to experience fatigue damage).

### Damage Analysis

The primary distresses in Jointed Plain Concrete Pavement (JPCP) include transverse cracking and faulting (NCHRP 2004). Damage analyses for transverse cracking (fatigue damage) and faulting were conducted to determine the relative pavement damages from various types of farm vehicles compared to those caused by a standard truck. The damage models for transverse cracking (fatigue damage) and faulting employed in the Mechanistic-Empirical Pavement Design Guide (MEPDG) were selected in this study (AASHTO 2008).

**Fatigue Damage Analysis.** In the MEPDG, the fatigue damage is computed by relating the ratio of MOR to applied stress to allowable number of load repetitions. The applied number of load applications ( $n_{i,j,k,l,m,n}$ ) is the actual number of axle type ( $k$ ) of load level ( $l$ ) that passed through traffic path ( $n$ ) under each condition of age, season, and temperature difference. The allowable number of load repetitions is the number of the load cycles at which fatigue failure is expected (corresponding to 50 percent slab cracking) and is a function of the applied stress and PCC strength. The allowable number of load repetitions is determined by the following fatigue model of MEPDG:

$$\text{Log}(N_{i,j,k,l,m,n}) = C_1 \times \left( \frac{MR_i}{\sigma_{i,j,k,l,m,n}} \right)^{C_2}$$

Where,

- $N_{i,j,k,\dots}$  = allowable number of load applications at condition  $i, j, k, l, m, n$
- $MR_i$  = PCC modulus of rupture at age  $i$ , psi
- $\sigma_{i,j,k,\dots}$  = applied stress at condition  $i, j, k, l, m, n$
- $C_1$  = calibration constant = 2.00
- $C_2$  = calibration constant = 1.22

As seen in this equation, the pavement fatigue damage could be characterized through allowable number of load repetitions ( $N_f$ ). The  $N_f$  of farm vehicles tested were estimated and compared with those for a standard 80-kip semi-truck. Maximum bending stresses at mid-slab edge bottom were calculated using ISLAB 2005 as critical responses for computing fatigue damage ( $N_f$ ).

Figure 7 **Error! Reference source not found.** compares fatigue damage predictions between cell 32 and cell 54 under fully loaded vehicle condition. As shown in Figure 7, the number of load repetitions to failure on cell 54 with 7.5 inch PCC slab is higher compared to cell 32 with five inch PCC slab for all farm equipment and standard semi-truck. As expected, PCC slab thickness has a significant effect on pavement service life. Figure 7 demonstrates that the representative farm vehicles fully loaded induced lower  $N_f$  (higher fatigue damage potential) than standard semi-truck. Among the farm vehicles, G1 exhibited the lowest number of repetitions to failure (i.e., highest fatigue damage potential).

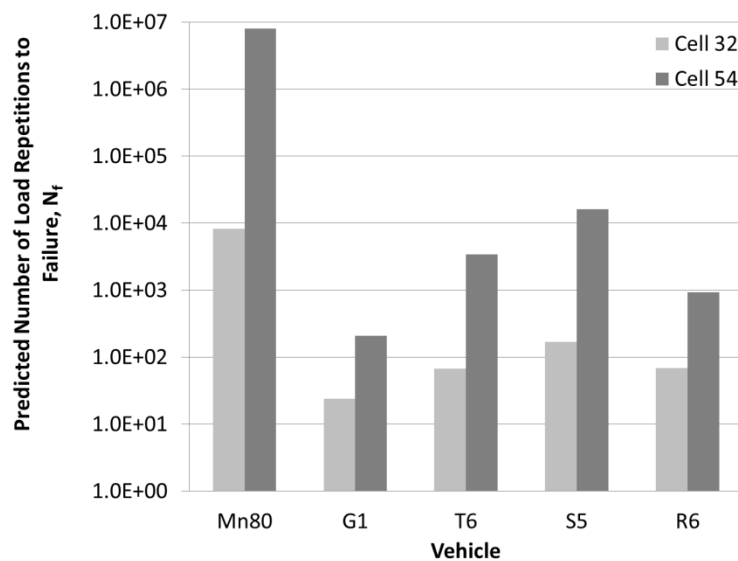


**Figure 7. Fatigue damage prediction comparisons between cell 32 and cell 54**

**Faulting Damage Analysis.** The MEPDG faulting damage model adopts an incremental approach to predict PCC transverse joint faulting (Khazanovich et al. 2004, NCHRP 2004). A faulting increment is determined for each month and the faulting level calculated in previous month affects the magnitude of increment for the next month. The faulting at each month is determined as a sum of faulting increments from all previous months in the pavement life since traffic opening.

The faulting damage model seems to indicate that the mean joint faulting at the end of month ( $m$ ) highly depends on the differential energy. The differential

energy (DE) is defined as the energy difference in the elastic subgrade deformation under the loaded slab (leave) and the unloaded slab (approach):

$$DE = k/2 \times (w_l + w_{ul}) \times (w_l - w_{ul})$$

Where,

- DE = differential energy of subgrade deformation
- $w_l$  = corner deflection under the loaded slab
- $w_{ul}$  = corner deflection under the unloaded slab
- $k$  = modulus of subgrade reaction

The faulting damage analysis was conducted in terms of DE which is the only variable calculated from available field data. DEs induced by each farm equipment are compared with those produced by a standard 80-kips semi-truck.

Figure 8 compares faulting damage predictions between cell 32 and cell 54 subjected to those five representative vehicles under fully loading condition. As seen in the figure, DEs on cell 32 is always greater than those on cell 54, regardless of vehicle type. Similar to fatigue damage analysis, G1, among all farm vehicles, produces the highest DE. This result indicates that G1 has the highest potential to cause faulting damage to rigid pavement system within the constraints of this study.

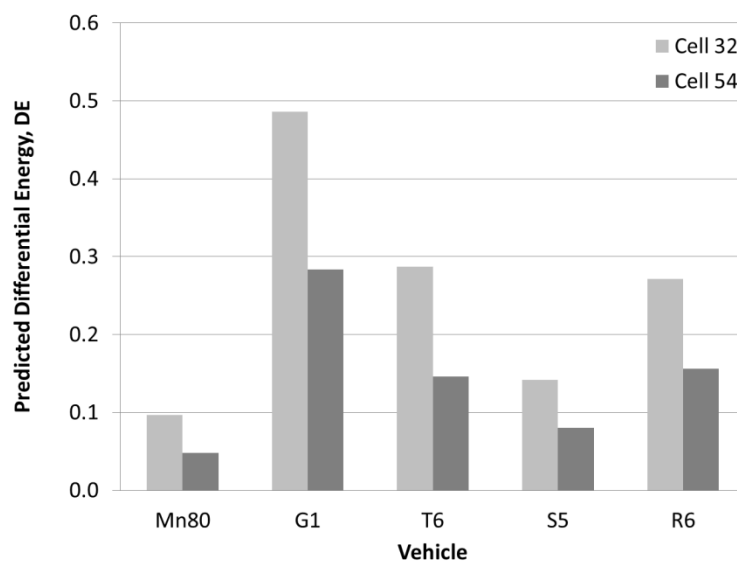


**Figure 8. Faulting damage prediction comparisons between cell 32 and cell 54**

### Discussion on Corner Crack

Severe corner cracks developed and became aggravated on cell 32 (see Figure 9) during Fall 2009, Spring 2010, and Fall 2010 field testing periods. It is likely that various factors including heavy loading of grain cart and large amount of load repetition might have contributed to these corner breaks. Based on field observation, the corner crack occurring in cell 32 could be attributed to the loss of subgrade support resulting from pumping of water with fine materials under heavy vehicle load repetition.



**Figure 9. Corner breaks on both side of the cell 32 concrete slab**

Corner cracks are diagonal cracks that meet both the longitudinal and transverse joint within six-ft., measured from the corner of the slab (Lee et al. 2002). The crack usually extends through the entire thickness of the slab. The main causes of corner breaks identified are load repetitions combined with loss of subgrade support, poor load transfer across the joint, and curling and warping stresses. Further investigations were conducted to identify the relative corner cracking damage caused by farm vehicles on cell 32 PCC slab using theoretical models (closed form equation and FE solution).

Ioannides et al. (1985) found that the maximum moment occurs at a distance of  $1.8 c^{0.32} l^{0.59}$  from corner in which  $c$  is the side length of a square contact area and  $l$  is the radius of the relative stiffness. The radius of the relative stiffness could be calculated as follows:

$$l = \left[ \frac{Eh^3}{12(1-\nu^2)k} \right]^{0.25}$$

Where  $E$  is the elastic modulus of concrete,  $h$  is the thickness of the slab,  $\nu$  is Poisson's ratio of concrete, and  $k$  is the modulus of subgrade reaction.

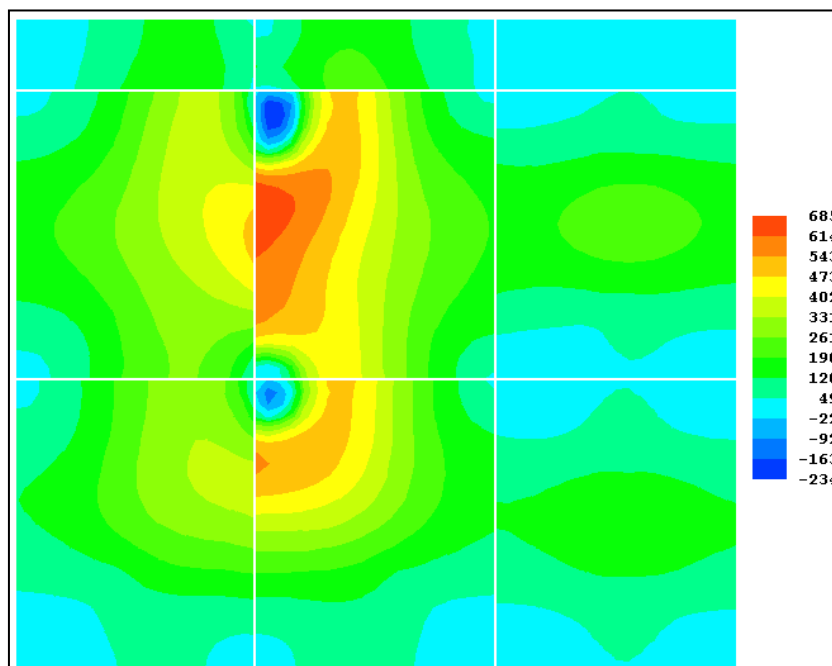
The closed-form equation (Ioannides et al. 1985) results and the ISLAB2005 results were compared for various representative farm vehicles to further investigate the relative corner cracking damage on cell 32. Farm vehicles, G1, R6, S5, and T6 under various temperature conditions of cell 32 were considered in these comparisons. The standard semi-truck, Mn80, was also selected as a control vehicle.

Table 2 summarizes calculated maximum bending stresses on the top of the slab when various representative vehicles load slab corner near transverse joint under different temperature conditions. As shown in Table 2, it is found that as the temperature gradient increases, the bending stresses on the top of the slab increases. Among all five representative vehicles, R6 and G1 produced the highest bending stresses at the top of the slab about 4.5 to 5 ft. away from the slab corner along the joint. Differences exist between the FE solutions and the closed equation results with respect to the location of maximum bending stresses. The FE solutions provide longer distances from corner in comparisons to closed form equation results. The ratios of FE solutions to closed form equation results for each vehicle are listed in Table 2.

**Table 2. Summary of maximum bending stresses on the top of the slab and their locations**

Vehicle	Max. bending Stress (psi)				Average distance from the corner, ft		a/b ratio
	Temperature Gradient (°F/in.)				FE solutions (a)	Closed form equation results (b)	
	0	-2	-4	-6			
Mn80	299	375	453	527	3.5	1.7	2.06
G1	429	505	595	685	4.5	2.4	1.88
R6	496	594	689	779	5.0	2.0	2.50
S5	365	442	523	599	3.5	1.6	2.19
T6	460	537	621	712	3.5	1.7	2.06

Figure 10 is a graphical representation of the FE calculated stress distribution for G1 at the top of cell 32 slab. As shown in Figure 10, the maximum bending stress is located at 4.5 ft away from the slab corner and there is a bending zone that propagates from the slab joint to the slab edge. This bending stress zone could eventually lead to corner cracking if the bending stress is high enough compared to PCC strength. Based on field observations, corner cracks only occurred on 2.5-ft away from the slab corner which is close to the distance calculated from the closed form equation. The bias in FE solutions compared to field observation could be attributed to the construction quality of the concrete and the use of approximations inherent to numerical modeling. The stress distribution in Figure 10 is just a concept for illustrative purposes than to prove that the corner crack occurred exactly at that point where the maximum bending moments are located at in this figure. This investigation also demonstrated that there is a very high possibility for corner cracking to occur if there is a temperature curling combined with heavy farm equipment loading at the slab corner.



**Figure 10. Cell 32 stress distribution caused by G1 on top of the PCC slab**

### Summary and Conclusions

The study reported in this paper evaluated the impact of farm vehicles on rigid pavement responses and damage using Finite Element (FE) analyses. Fatigue and faulting damage analyses were conducted by employing MEPDG distress prediction models. The study findings are summarized as follows:

- A fully loaded 1,000-bushel grain cart (G1) caused the highest fatigue and faulting damage to rigid pavement sections. This is attributed to the heavy axle weight of the vehicle as it has only one rear axle to distribute the heavy loading.
- The damage caused by farm equipment is governed by their axle weight rather than the gross vehicle weight.
- Increases in slab thickness and subgrade strength are some very important measures to prevent early failure of rigid pavements caused by farm vehicles.
- There is a very high possibility for corner cracking to occur if there is temperature curling combined with heavy farm equipment loading at the PCC slab corner.

In this study, the corner cracking observed in cell 32 could be attributed to the loss of subgrade support resulting from pumping of water along with fine materials under repeated heavy vehicle loading. The results of theoretical models (closed form equation and FE solution) also indicate that corner loading could introduce higher bending stress at the top of the slab and thus cause the occurrence of corner crack.

In conclusion, all farm vehicles introduce different levels of damage to PCC pavements. Vehicle loading/configurations, PCC slab thickness, slab length, modulus of subgrade reaction, and environmental conditions are all important factors that should be considered in the analysis and design of rigid pavements subjected to farm equipment loading.

### **Acknowledgements**

The authors wish to acknowledge industries represented by Professional Nutrient Applicators Association of Wisconsin (PNAAW), Iowa DOT/Iowa Highway Research Board, Minnesota Local Road Research Board (LRRB), Minnesota DOT, and Illinois DOT for sponsoring this study. The authors also acknowledges the private industries, Wisconsin manure applicator association, John Deere, Professional Dairy Producers of Wisconsin, Husky Farm Equipment, Minnesota Custom Manure Applicator Association and Michelin Tire, for sponsoring this study and providing testing equipment. The authors also extended their thanks to those undergraduate and graduate students from Iowa State University and University of Minnesota who helped in data collection during field testing.

### **References**

- NCHRP. (2004). *Guide for Mechanistic-empirical design of new and rehabilitated pavement structures*. Final Report, NCHRP Project 1-37A, Transportation Research Board, National Research Council, Washington, DC.
- AASHTO (2008). *Mechanistic-Empirical Pavement Design Guide: A Manual of Practice*. American Association of State Highway and Transportation Officials, Washington, DC.
- De Young, C. (1966). "Spacing of undoweled joints in plain concrete pavement." *Highway Research Record 112*, 46-54.
- Fanous, F. C., Coree, B., and Wood, D. (1999). *Response of Iowa Pavements to Heavy Agricultural Loads*. Ames, IA: Iowa Department of Transportation.
- Hiller, J. (2007). *Development of Mechanistic-Empirical Principles For Jointed Plain Concrete pavement Fatigue Design*. Champaign, IL: University of Illinois at Urbana-Champaign.
- Huang, Y. (1993). *Pavement Analysis and Design*. Englewood Cliffs, NJ: Prentice-Hall, Inc.
- Ioannides, A. T., Thompson, M. R., and Barenberg, E. J. (1985). "Westergaard solutions reconsidered." *Transportation Research Record 1043*, 13-23.
- Lim, J., Azary, A., Khazanovich, L., Wang, S., Kim, S., Ceylan, H., and Gopalakrishnan, K. (2011). *Effects of Implements of Husbandry (Farm Equipment) on Pavement Performance*. Draft of final report (In press), Maplewood, MN: Minnesota Department of Transportation.
- Khazanovich, L., Shats, E., Yu, T., Rao, S., Galasova, K., Gotlif, A., and Mallela, J. (2005). *ISLAB2005 (Version 1.1 Standard) [Computer Software]*. Applied Research Associates, Inc. Available from [www.ara.com/](http://www.ara.com/)
- Khazanovich, L., Darter, M. I., and Yu, H. T. (2004). "Mechanistic-empirical model to predict transverse joint faulting." *Transportation Research Record 1896*, 34-45.

Lee, Y. L., Lee Y.M. and Yen S. T. (2002). "Corner loading and curling stress analysis for concrete pavements - an alternative approach." *Canadian Journal of Civil Engineering*, 29 (4), 576-588.

Oman, M. V., Deusen, D. V., and Olson, R. (2001). *Scoping Study: Impact of Agricultural Equipment on Minnesota's Low Volume Roads*. Maplewood, MN: Minnesota Department of Transportation.

Sebaaly, P. E., Siddharthan, R., El-Desouky, M., Pirathapan, Y., Hitti, E., and Vivekanathan, Y. (2002). *Effect of Off-Road Tires on Flexible & Granular Pavements*. Pierre, SD: South Dakota Department of Transportation.

Snyder, M. (2008). *Lessons Learned From Mn/ROAD (1992-2006): Final Report*. American Concrete Pavement Association.

Wang, S. (2011). *The Effects of Implements of Husbandry Farm Equipment on Rigid Pavement Performance*. M.S. Thesis. Ames, IA: Iowa State University.